

3D Sonoembryology

Ritsuko K Pooh

Clinical Research Institute of Fetal Medicine (CRIFM) and Perinatal Medicine Clinic (PMC), Osaka, Japan

Correspondence: Ritsuko K Pooh, Clinical Research Institute of Fetal Medicine (CRIFM) and Perinatal Medicine Clinic (PMC) 7-3-7, Uehommachi, Tennoji, Osaka 543-0001, Japan, Phone: +81-6-6775-8111, Fax: +81-6-6775-8122, e-mail: rkpooh@me.com

ABSTRACT

After the introduction of high-frequency transvaginal transducers in clinical obstetrics, the term 'sonoembryology' was first coined in 1990.¹ Three-dimensional sonography performed with a transvaginal approach has expanded the depth of inquiry and allowed three-dimensional sonoembryology.

Transvaginal approach combined with high frequency (12 MHz) and a harmonic phase inversion method can provide us images with high quality and high resolution demonstrating detailed embryonal structures, including normal development of embryos and fetuses, and many congenital abnormalities, such as conjoined twin from 9 weeks, vertebral abnormality from 9 weeks, cleft lip/palate from 12 weeks, congenital cataract from 14 weeks, limb abnormality from 11 weeks, thoracoabdominal abnormality from 12 weeks of gestation.

It is possible that by developing 3D neurosonoembryology imaging *in utero*, current fetal staging (which uses gestational age based on last menstrual period or crown-rump length measurement) may change into a 'morphological staging system', such as the Carnegie staging system, which has been central to embryology.

A novel imaging technique of high-resolution transvaginal 3D sonography is illustrated in the definition of normal embryonic anatomy as well as in the identification of many congenital anomalies. They allow extending the detection of anatomical congenital anomalies to an earlier gestational age.

Keywords: Sonoembryology, Three-dimensional ultrasound, Fetus, First trimester.

INTRODUCTION

After the introduction of high-frequency transvaginal transducers in clinical obstetrics, the term 'sonoembryology' was first coined in 1990.¹ Three-dimensional sonography performed with a transvaginal approach has expanded the depth of inquiry and allowed three-dimensional sonoembryology.²

A major limitation of embryology is that it has been traditionally based in specimens obtained after embryonic death. Structural and functional early human development has been able to be assessed by three-dimensional and four-dimensional sonography.³ Modern imaging techniques allow the definition of *in vivo* anatomy, including visualization of the embryonic circulation and dynamic feature, which could not be characterized in fixed specimens.⁴

In this article, we will illustrate 3D sonoembryology with recent advances of three-dimensional visualization *in utero* as the anatomical counterparts with three-dimensional anatomy.

Visualization of Normal Embryos by 3D Ultrasonography

3D images of embryos were generated using the high-frequency transvaginal transducer (Voluson® E8 with 6 to 12 MHz/256 element 3D/4D transvaginal transducer, GE Health care, Milwaukee, USA). Transvaginal approach, combined with high frequency of 12 MHz with a harmonic phase inversion method, can provide us images with high quality and high resolution demonstrating detailed embryonal structures. We have examined over 500 normal embryos/fetuses in the first trimester by this method.

Figure 1 shows a gestational sac at 4 weeks of gestation (menstrual age), and the yolk sac was visualized at 5 weeks. Demonstration of an embryo of less than 10 mm (greatest length) has been difficult in the past and not visualized in detail. Figure 2 illustrates the development of the spinal cord at embryonal size of 5.5 mm, 18.3 mm and 26.3 mm.⁴ Thereafter, the vertebral bony structure can be visualized from 11 weeks of gestation, and gradual closure of the bilateral laminae caudally from the cervical region downward.

The development of the embryonic circulation became visualized by 3D power Doppler imaging technology.³ Figure 3 illustrates the vascular network of an embryo at 9 weeks of gestation. In 1993 and 1994, color Doppler detection and assessment of brain vessels in the early fetus using a transvaginal approach was reported.^{5,6} Clear visualization by transvaginal power Doppler of the common carotid arteries, internal and external carotid arteries and middle cerebral arteries at 12 weeks of gestation was reported in 1996.⁷ By using 3D power Doppler technology, the vascular anatomy can now be imaged clearly by identification of the common carotid arteries, internal carotid arteries, circle of Willis and middle cerebral arteries (Fig. 4).

The utilization of postprocessing algorithms, such as maximum mode can be used to demonstrate the fetal skeleton. Chaoui et al⁸ reported clear 3D images for the identification of an abnormally wide metopic suture in the second trimester of pregnancy. However, rapid ossification of the craniofacial bones occurs during the first trimester of pregnancy. We demonstrate in this paper, the identification of the craniofacial skeleton from 10 weeks of gestation onwards. Figures 5 and 6 show early fetal craniofacial bony structures at 11 and 14 weeks respec-

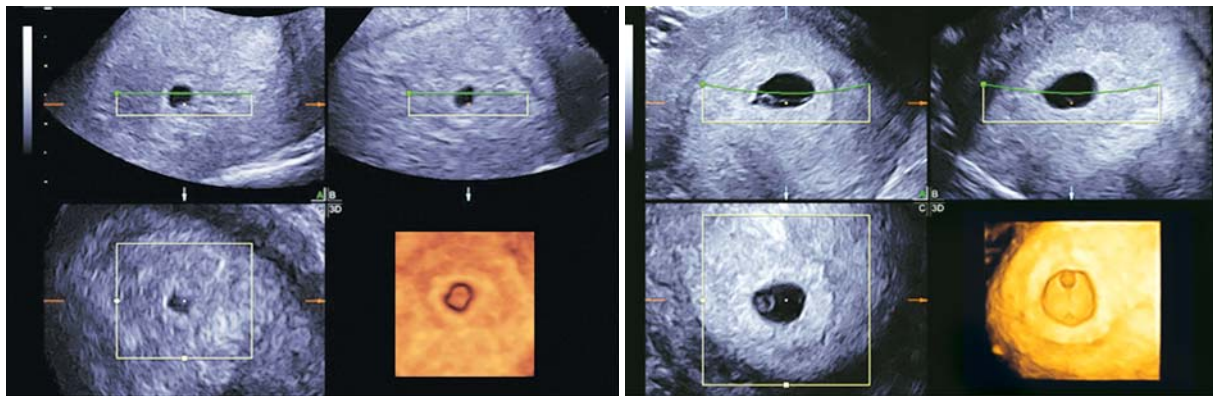


Fig. 1: Development of gestational sac (4 and 5 weeks of gestation). (left) 4 weeks (2 weeks after conception) of gestation. Three orthogonal view and 3D constructed image demonstrated early gestational sac. (right) The beginning of 5 weeks, yolk sac is detectable inside gestational sac

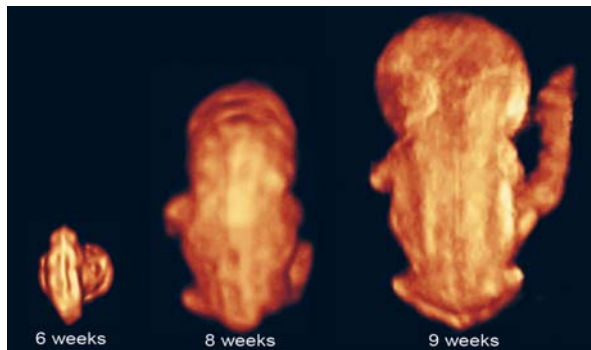


Fig. 2: 3D reconstructed image of the embryo (6-9 weeks of gestation). Embryonal sizes are 5.5, 18.3 and 26.3 mm. At 9 weeks of gestation, the spinal cord is demonstrated as a thin line, compared with that at 8 weeks of gestation

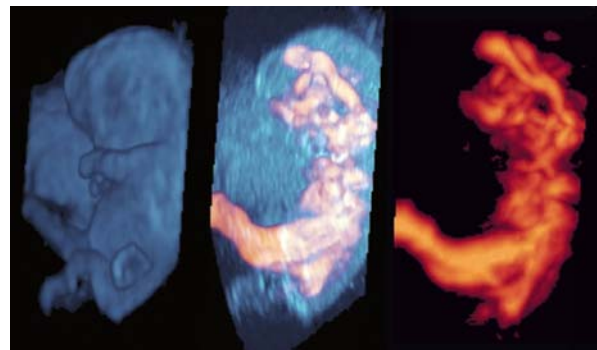


Fig. 3: Early vascular system at 9 weeks of gestation. (left) 3D gray mode. (middle) 3D power Doppler with surface appearance. (right) 3D power Doppler image

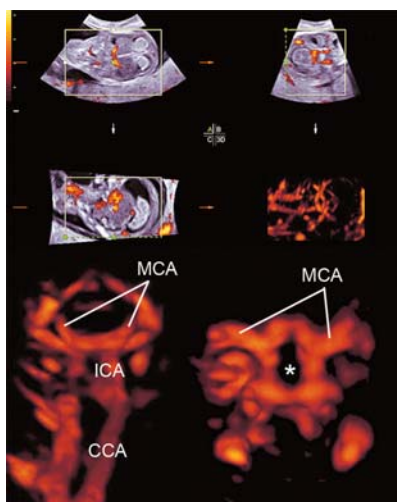


Fig. 4: Premature vascularity of normal 12-week brain. (upper) Three orthogonal view of power Doppler image and 3D reconstructed image (front-back view of A plane). (lower left) Front-back image of common carotid arteries (CCA), internal carotid arteries (ICA) and brain basilar arteries. MCA; middle cerebral artery. (lower right) 3D image from fetal parietal direction. The circle of Willis (asterisk) is clearly visualized

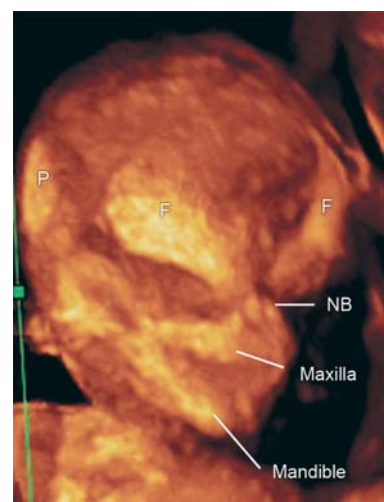


Fig. 5: 3D maximum mode image of normal craniofacial structure at 11 weeks of gestation. Premature bony structure of frontal bone (F), parietal bone (P), nasal bone (NB), maxilla and mandible are recognizable

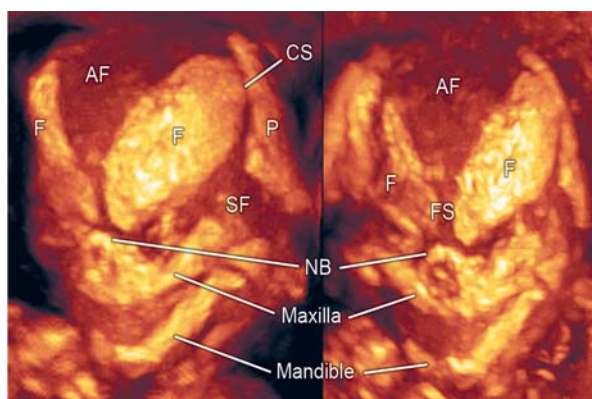


Fig. 6: 3D maximum mode image of normal craniofacial structure at 14 weeks of gestation. (left) Oblique view, (right) frontal view. Anterior fontanelle (AF), sphenoidal fontanelle (SF), frontal suture (FS), coronal suture (CS), nasal bone (NB), maxilla and mandible are gradually formed according to cranial bony development

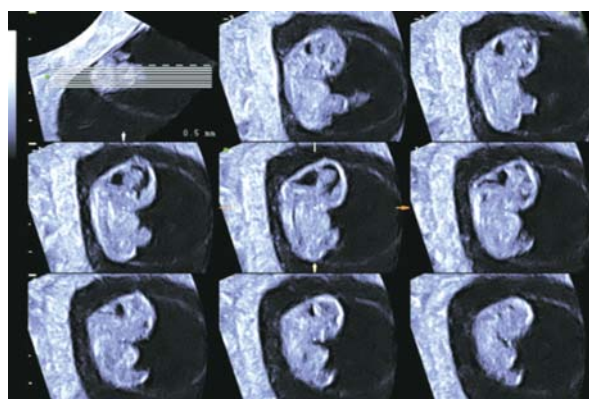


Fig. 8: Tomographic sagittal imaging of normal fetus at the beginning of 8 weeks of gestation

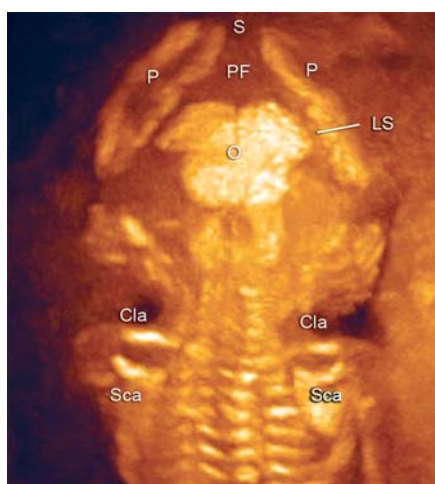


Fig. 7: 3D maximum mode image of occipital view at 13 weeks of gestation. Note the premature occipital bone appearance. Midline crack is demonstrated. S; Sagittal suture, P; Parietal bone, PF; Posterior fontanelle, O; Occipital bone, Cla; Clavicula, Sca; Scapula, LS; Lambdoid suture

tively, using the maximum mode algorithm. The difference of frontal bone morphology between 11 and 14 weeks demonstrates membranous ossification of the cranium at this stage. Figure 7 demonstrates the structure of the skull in the occipital region at 13 weeks of gestation.

During the early embryonic period, the central nervous system anatomy rapidly changes in appearance. 3D sonography using transvaginal sonography with high-resolution probes allows imaging of early structures in the embryonic brain. Figures 8 to 10 demonstrate fetal brain detailed morphology between 8th and 10th week, and this can be accomplished through the use of three orthogonal planes and “tomographic ultrasound imaging”. Serial examinations allow obtaining similar sections of the fetal brain at different stages of development. Therefore, it is possible to document the changes in CNS development as demonstrated in Figure 11. Recent reports published on embryonal ventricular development from

6th or 7th week by use of 3D inversion rendering mode, have made sonoembryology more sophisticated and objective.^{9,10} It is possible that by developing 3D neurosonoembryology imaging *in utero*, current fetal staging (which uses gestational age based on last menstrual period or crown-rump length measurement) may change into a ‘morphological staging system’, such as the Carnegie staging system, which has been central to embryology.

Thoracoabdominal structures can also be imaged in the first trimester. For example, Figure 12 shows tomographic ultrasound imaging of fetal chest and abdomen at 13 weeks of gestation. Clear visualization of the lung-liver interface can be of value in the early diagnosis of thoracoabdominal abnormalities, such as a diaphragmatic hernia.

Prenatal Diagnosis of Anatomical Congenital Anomalies in the Human Embryo

The prenatal diagnosis of congenital anomalies with ultrasound is based upon identification of a substantial departure of normal anatomy. This has been possible in the second and third trimester of pregnancy, and this achievement has made the diagnosis of congenital anomalies one of the objectives of modern prenatal care. The definition of the “normal anatomy” of the human embryo provides the basis for the identification of congenital anomalies at the earliest stages of human development. This goes beyond the mere identification of nuchal translucency, because it is now possible to identify anomalies even in the absence of an abnormal nuchal translucency. Therefore, the scope of prenatal diagnosis during embryonic life has been widened by sonoembryology with 3D ultrasound.

Conjoined Twins

Conjoined twins are defined as monozygotic-monoamniotic twins fused at any portion of their body as a result of an incomplete division of the embryonic disk after the 13th day of conception. Pathogenesis of the condition is considered as the result from failure of complete separation. Careful observation in the first trimester can reveal this condition from the early pregnancy. Figure 13 demonstrates conjoined twins with limb body-wall complex at 9 weeks of gestation. Three-dimensional ultrasound can objectively depict this rare abnormality.

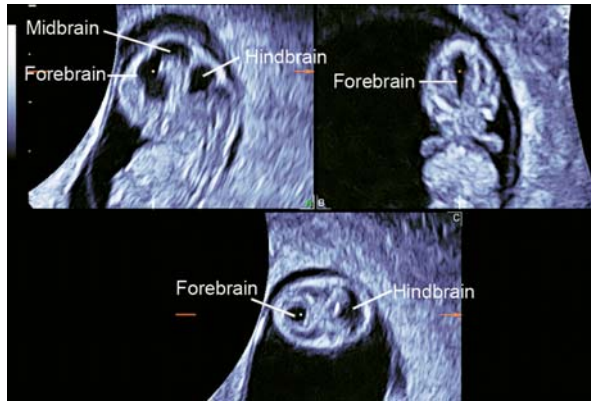


Fig. 9: Three orthogonal image of normal brain at the end of 8 weeks of gestation. The development of premature ventricular system is seen. Note the different appearance from the beginning of 8 weeks of gestation (Fig. 17)

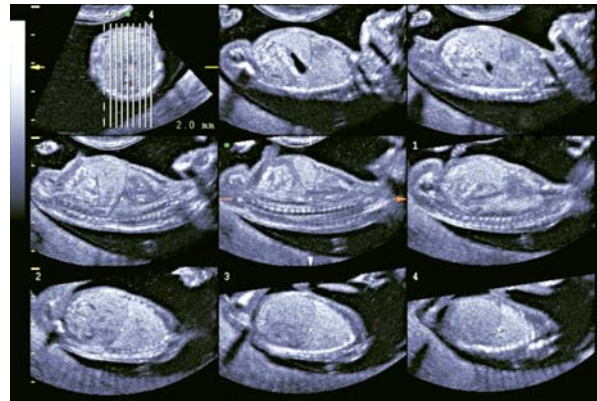


Fig. 12: Tomographic ultrasound imaging of normal thoracoabdominal structure at 13 weeks of gestation. Parallel sagittal sections are shown. Lung-liver border and intra-abdominal organs are clearly visualized

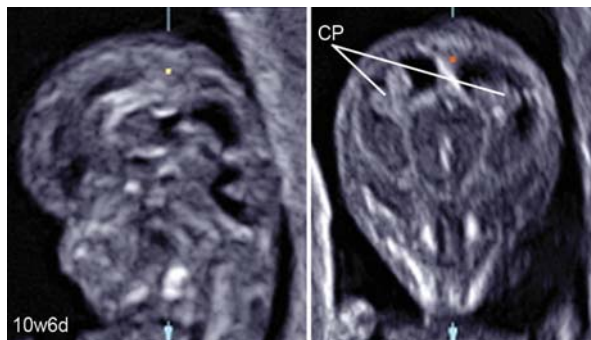


Fig. 10: Sagittal section and coronal sections of 10-week fetus. CP; Choroid plexus of the lateral ventricles

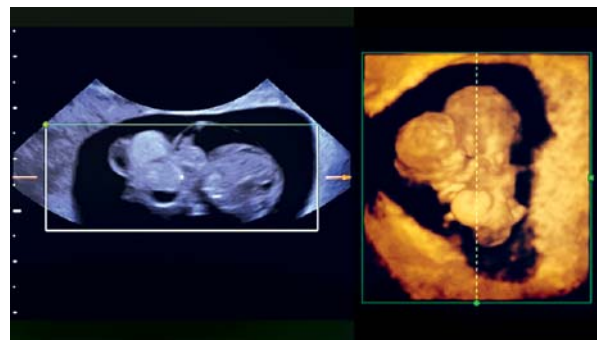


Fig. 13: Conjoined twins with limb body-wall complex at 9 weeks of gestation. Two heads and one body are obviously demonstrated. Liver and other abdominal organs were prolapsed

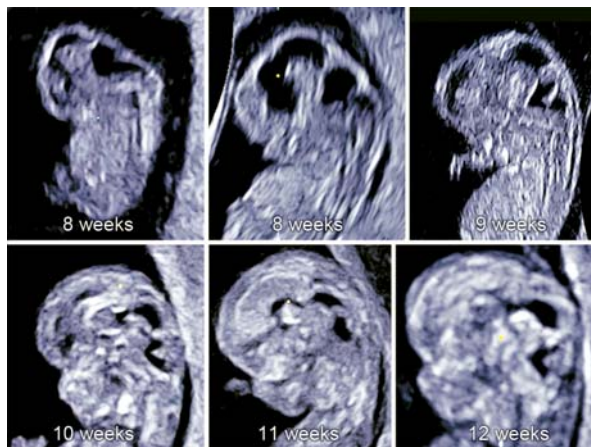


Fig. 11: Normal brain development by mid-sagittal 3D US section between 8 and 12 weeks of gestation

Vertebra and Spinal Cord Anomaly

Spina bifida is the most common congenital spinal cord anomaly. It is often detected during the second and third trimesters. However, the fundamental basis for this anomaly is a failure of the neural tube to close during early embryonic age.

Most reports of the diagnosis of spina bifida *in utero* have occurred after 12 weeks of gestation. Blaas et al¹¹ reported an early diagnosis using 2D and 3D ultrasound before 10 weeks of gestation. Figure 14 shows the early diagnosis of spina bifida in a case of OEIS complex (omphalocele, bladder exstrophy, imperforate anus, spina bifida) at 9 weeks of gestation. Iniencephaly is a rare neural tube defect that combines extreme retroflexion (backward bending) of the head with severe defects of the spine, associated with acrania, anencephaly and encephalocele. The prognosis for those with iniencephaly is extremely poor. Early detection of iniencephaly is possible (Fig. 15). Scoliosis is often associated with limb body-wall complex, and rarely scoliosis is associated with early vertebral fusion as shown in Figure 16. Extreme hyperdorsiflexion (backward bending) is a rare finding with unknown clinical significance. Figure 17 demonstrates extreme hyperdorsiflexion seen in a case of trisomy 21.

Facial Abnormalities

A facial anomaly can be associated with a central nervous system anomaly (e.g. holoprosencephaly), be an isolated finding or part

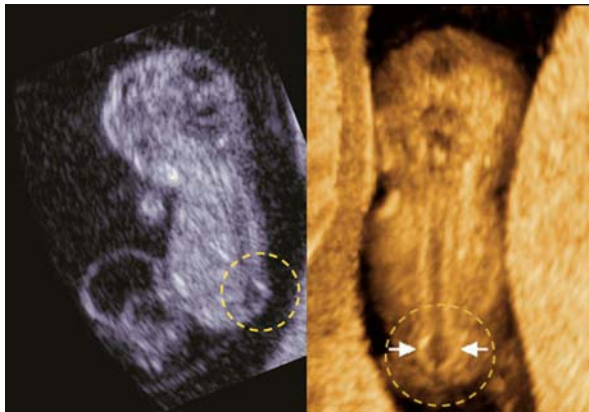


Fig. 14: Spina bifida at 9 weeks of gestation. Left; 2D sagittal image. Cystic formation was seen (white circle) at lumbar part. Right; 3D image of neural tube. Clear dilatation of the neural tube is demonstrated (arrows)



Fig. 17: Extreme hyperdorsiflexion seen in a case of trisomy 21 at 14 weeks of gestation. Left upper and right; 3D reconstructed oblique anterior and lateral views of the fetus. Left lower; 3D maximum mode demonstrating bony structure

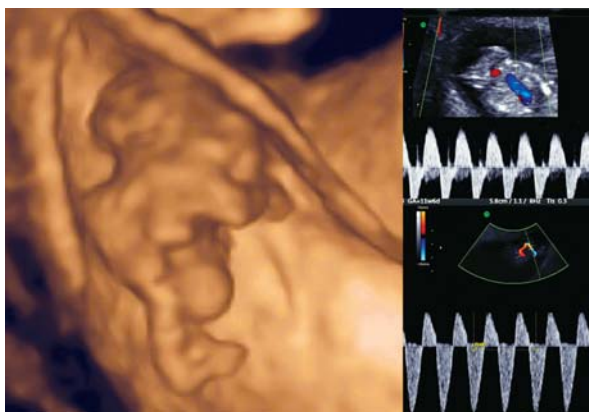


Fig. 15: Iniencephaly at 12 weeks of gestation. Left; 3D reconstructed image. Acrania, short body with dorsoflexion are well-demonstrated. Right; This fetus had reverse flows of descending aorta (right upper) and umbilical artery (right lower) and intrauterine fetal demise was confirmed one week later

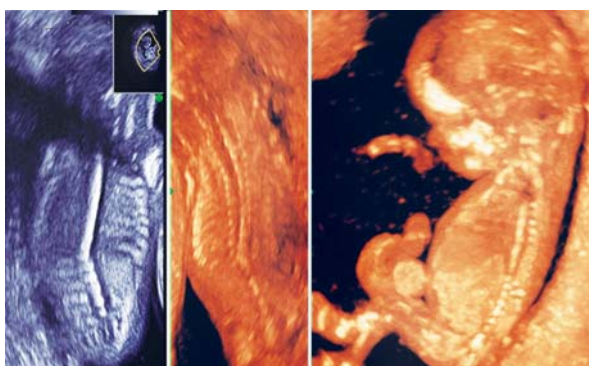


Fig. 16: Fused thoracic vertebral body with scoliosis at 13 weeks of gestation. Left; 2D sagittal image. Thoracic vertebral body is completely fused while lumbar vertebral bodies are apart. Middle; 3D maximum mode of dorsal view. Right; 3D maximum mode of lateral view

of a syndrome. Detection of the presence or absence of a nasal bone has been found to be of value in the assessment of aneuploidy in the first trimester of pregnancy (risk assessment

for trisomy 21).¹²⁻¹⁶ Cicero and her colleagues reported that the nasal bone was absent in 113 (0.6%) of the 20,165 chromosomally or phenotypically normal fetuses and in 87 (62.1%) of the 140 fetuses with trisomy 21.¹⁶ 3D sonography allows a midsagittal section of the fetal face to be obtained by utilizing the three orthogonal planes, and avoids the pitfall of obtaining a parasagittal view, which could lead to false-negative results. Tomographic ultrasound imaging also allows demonstration of facial midline structures in detail, by examining close parallel sections (Fig. 18). It is important to be aware that the quality of the orthogonal planes is dependent upon the original plane of acquisition. Rembouskos et al¹⁷ have expressed some reservations about the use of 3D for nasal bone assessment.

Benoit and Chaoui¹⁸ described the diagnosis of bilateral or unilateral absence or hypoplasia of nasal bones in second trimester screening for Down syndrome by using 3D sonography with maximal mode rendering. Figure 19 shows the midsagittal section of fetal face, craniofacial bony reconstructed image of normal fetus and trisomy 21 fetuses in the first trimester.

A short maxillary length has been associated with trisomy 21.¹⁹ Micrognathia can be detected as an isolated structural anomaly, as one of the features of a chromosomal abnormality or a syndrome.²⁰ Assessment of the facial features, chin development and mandibular size by 3D ultrasound in the second and third trimesters has been reported.²¹ By using the surface mode and maximum mode (Fig. 20), the fetal profile and facial bone structure in normal and abnormal fetuses can be described in the first trimester.

Cleft lip and palate is usually demonstrated and diagnosed in the second and third trimesters. However, recent advances of the transvaginal 3D ultrasound have provided accurate and informative diagnostic images of cleft lip with orientation of left-sided, right-sided or bilateral cleft lip (Fig. 21). Furthermore, the palate is still created during pregnancy, but 3D reconstructed image can demonstrate cleft palate as shown in Figure 22. Up-to-date tomographic ultrasound imaging can provide the precise

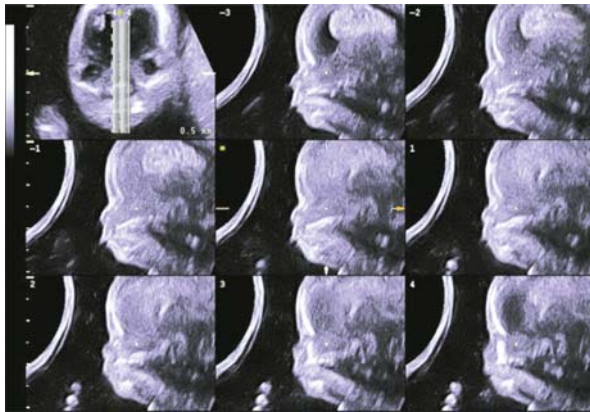


Fig. 18: Tomographic ultrasound image of fetal profile with hypoplastic nasal bone at the end of 13 weeks of gestation. Thinly sliced parallel cutting section of midsagittal plane shows fetal profile in detail and hypoplastic nasal bone

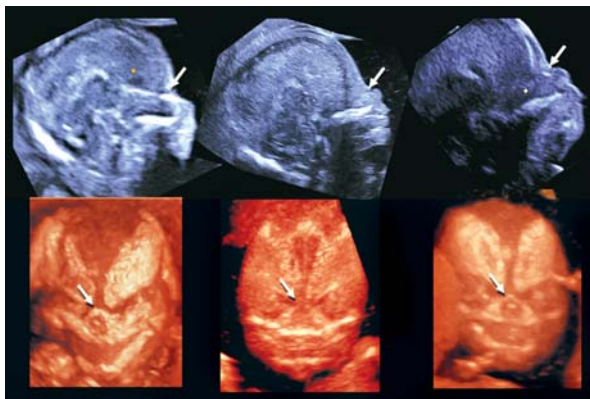


Fig. 19: Midsagittal 2D image of fetal profile and craniofacial bony reconstructed image of normal fetus (left) and trisomy 21 fetuses (middle and right) at 13 to 14 weeks of gestation. (left) Normal fetus. Nasal bone is clearly visualized in both 2D and 3D images (arrows). (middle) Nasal bone defect in a case of trisomy 21. Nasal bone is completely missing in both 2D and 3D. (right) Nasal bone hypoplasia in a case of trisomy 21. Small nasal bone is visualized in both 2D and 3D

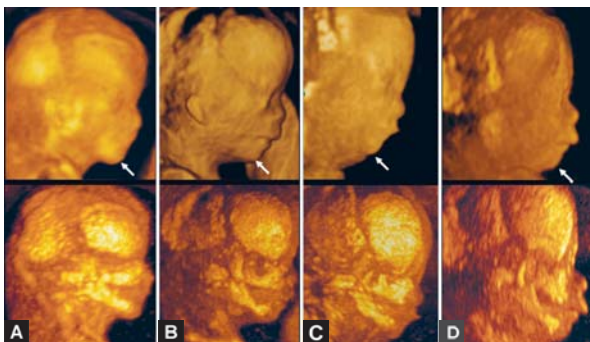


Fig. 20: Fetal profile and facial bone development in normal fetus (A) and abnormal fetuses (B to D) at 12 to 13 weeks of gestation. A; Normal fetus, B; Trisomy 21 fetus, C; Trisomy 18 fetus, D; Mild micrognathia with normal chromosome. Lateral views of fetal profile (upper figures) show the difference of chin angle. Maximum mode images (lower figures) indicate the hypoplastic maxilla and mandible in B to D

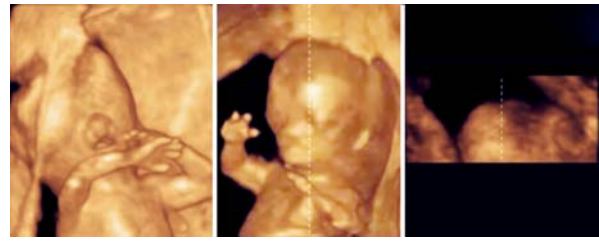


Fig. 21: Bilateral and unilateral cleft lip seen at 12 weeks of gestation. Left and middle; 3D reconstructed images of bilateral cleft lip seen in cases of trisomy 18 (left) and trisomy 21 (middle). Right; 3D reconstructed image of unilateral cleft lip seen as a single finding

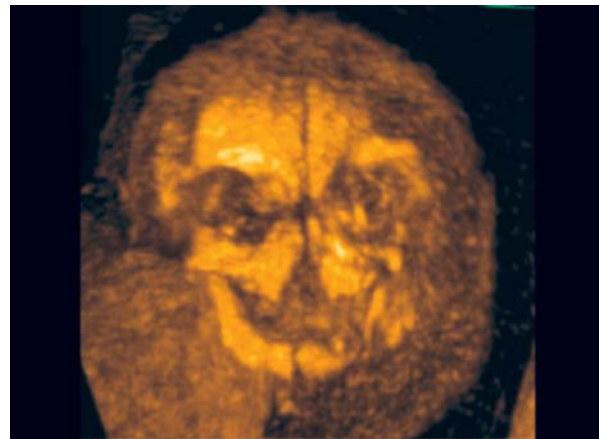


Fig. 22: Cleft plate at 14 weeks of gestation. 3D maximum mode demonstrating midline large cleft of maxilla

demonstration of palate shown in Figure 23 and the possibility of early diagnosis of cleft palate.

Eyeballs and lenses are detectable by ultrasound from the late first trimester. Cataract is defined by the presence of any lens opacity. The incidence of congenital cataract ranges from 1 to 6 newborn infants out of 10,000 births.²² Cataract development is strongly linked to the embryonic ocular development. The lens differentiates from the surface ectoderm before the 6th week of gestation, explaining the absence of cataract in case of late first-trimester fetal infection.^{23,24} A genetic cause is responsible for 30% of unilateral cataracts and 50% of bilateral cataracts. Prenatal diagnosis of fetal cataract was reported in the late second and third pregnancy.²⁵⁻²⁹ Figure 24 shows fetal bilateral cataract with microphthalmia as early as 14 weeks of gestation.

Limb Abnormalities

Limb abnormalities can occur as isolated findings or as one component of a syndrome or sequence. However, only 5% of congenital hand anomalies occur as part of a recognized syndrome.³⁰ Overlapping fingers, wrist contracture (Fig. 25) and forearm deformities are often associated with a chromosomal abnormality, such as trisomy 18. Most skeletal anomalies are recognizable in the second trimester. However,

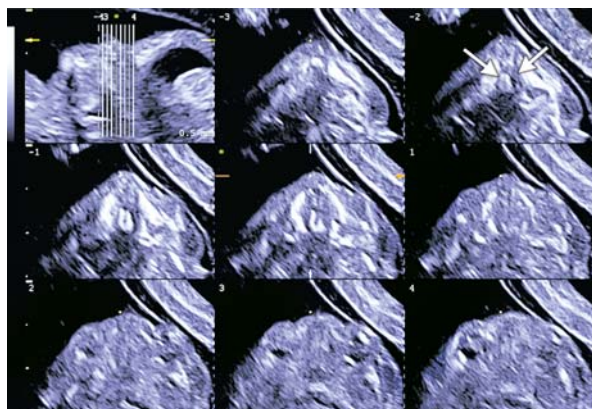


Fig. 23: Tomographic ultrasound imaging of cleft palate at 12 weeks of gestation. Bilateral cleft palate is demonstrated (arrows)

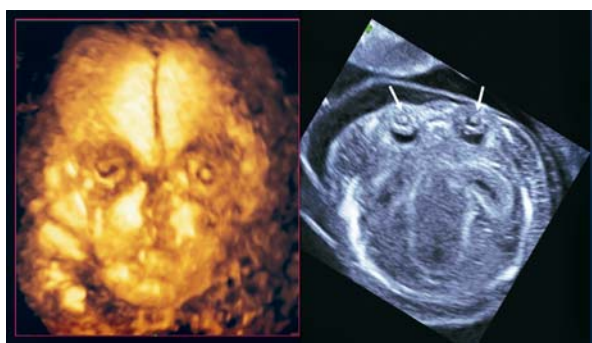


Fig. 24: Congenital cataract at 14 weeks of gestation. Bilateral congenital cataract is demonstrated as lens opacity (arrows) in 3D (left) and 2D (right) images



Fig. 26: Short limb abnormality at 13 weeks of gestation. Short lower extremities with large abdomen is clearly demonstrated in the frontal (left) and lateral (right) views



Fig. 27: Upper limb abnormality at 11 weeks of gestation. 3D ultrasound revealed contracted elbow joint abnormality. Right figures show macroscopic appearance of upper limbs of aborted fetus

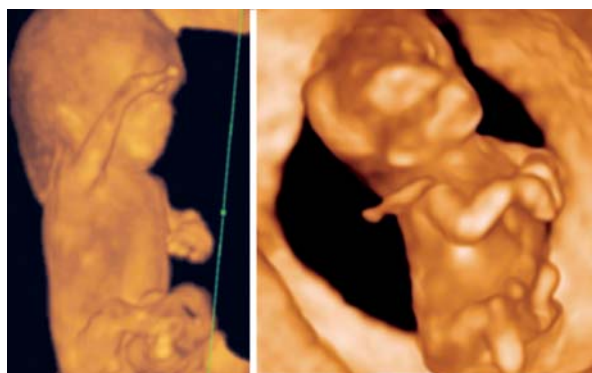


Fig. 25: Mild to moderate wrist contracture seen in cases of trisomy 18 at 12 to 13 weeks of gestation. Left; Mild wrist contracture is seen. Right; moderate wrist contracture is seen. Trisomy 18 was confirmed by chorionic villi sampling

several reports on congenital skeletal abnormalities (such as sirenomelia and others) in the first trimester have been documented.³¹⁻³⁵ Short limb abnormality in the first trimester was shown in Figure 26.

Figure 27 shows an 11 weeks fetus on 3D sonography with skeletal dysplasia of the bilateral upper extremities and normal lower extremities.



Fig. 28: Polydactyly and syndactyly at 14 weeks of gestation. 3D reconstructed ultrasound images clearly depicted bilateral polydactyly (upper) and left poly-/syndactyly (lower). Both cases were associated with holoprosencephaly

Finger abnormalities, such as polydactyly, oligodactyly and syndactyly, are detectable from the late first-trimester. In Figure 28, polydactyly and syndactyly at 14 weeks in cases of holoprosencephaly are well-demonstrated by 3D ultrasound.

Thoracoabdominal Abnormalities

Congenital diaphragmatic hernia (CDH) occurs in one of every 2000 to 4000 live births and accounts for 8% of all major congenital anomalies.³⁶ There are three types of CDH; posterolateral or Bochdalek hernia (occurring at approximately 6 weeks of gestation), the anterior Morgagni hernia and a hiatus hernia. The left-sided Bochdalek hernia occurs in approximately 90% of cases. Left-sided hernias allow herniation of both small and large bowel as well as intra-abdominal solid organs into the thoracic cavity. Early diagnosis of CDH in the first trimester has been reported.³⁷ Figure 29 shows the thoracoabdominal area of a fetus with a congenital diaphragmatic defect where the lung-liver border line acutely changes its angle from 13 to 15 weeks due to progressive liver upward movement into the chest. Early diagnosis of this defect is important.³⁷

Omphalocele is often seen from the first trimester. Physiological umbilical hernia is usually observed around 8-10 weeks of gestation, however, umbilical hernia seen after the beginning of 12 weeks is definitely pathological (Fig. 30).



Fig. 29: Congenital diaphragmatic defect at 13 and 15 weeks of gestation. Referral case due to nuchal translucency of 3 mm at 11 weeks of gestation. (Left) frontal view at 13 weeks. Dextrocardia (H), liver-up (Li) and oppressed left lung (Lt L) are demonstrated. (Right) frontal view at 15 weeks. The line of lung-liver border indicates acute angle changing in a short period due to progressive liver-up

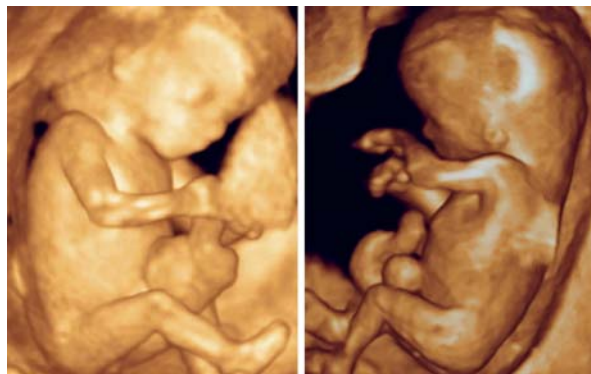


Fig. 30: Omphalocele at 12 to 13 weeks of gestation. 3D reconstructed ultrasound images clearly demonstrates omphalocele. Trisomy 18 was confirmed by chorionic villi sampling in both cases

CONCLUSION

A novel imaging technique of high-resolution transvaginal 3D sonography is illustrated in the definition of normal embryonic anatomy as well as in the identification of many of congenital anomalies. They allow extending the detection of anatomical congenital anomalies to an earlier gestational age.

ACKNOWLEDGMENTS

The author thanks the members of Global Ultrasound, Information Technologies, Women's Healthcare and Specialty of General Electrics Healthcare (Milwaukee, USA) for their technical support and collaboration in exploring the use of this equipment to advance the knowledge of sonoembryology.

REFERENCES

1. Timor-Tritsch IE, Peisner DB, Raju S. Sonoembryology: An organ-oriented approach using a high-frequency vaginal probe. *J Clin Ultrasound* 1990;18:286-98.
2. Benoit B, Hafner T, Kurjak A, Kupesic S, Bekavac I, Bozek T. Three-dimensional sonoembryology. *J Perinat Med* 2002;30:63-73.
3. Kurjak A, Pooh RK, Merce LT, Carrera JM, Salihagic-Kadic A, Andonotopo W. Structural and functional early human development assessed by three-dimensional and four-dimensional sonography. *Fertil Steril* 2005;84:1285-99.
4. Pooh RK, Shiota K, Kurjak A. Imaging of the human embryo with magnetic resonance imaging microscopy and high-resolution transvaginal three-dimensional sonography: Human embryology in the 21st century. *Am J Obstet Gynecol* Jan 2011: in print.
5. Kurjak A, Zudenigo D, Predanic M, Kupesic S. Recent advances in the Doppler study of early fetomaternal circulation. *J Perinat Med* 1993;21:419-39.
6. Kurjak A, Schulman H, Predanic A, Predanic M, Kupesic S, Zalud I. Fetal choroid plexus vascularization assessed by color flow ultrasonography. *J Ultrasound Med* 1994;13:841-44.
7. Pooh RK, Aono T. Transvaginal power Doppler angiography of the fetal brain. *Ultrasound Obstet Gynecol* 1996;8:417-21.
8. Chaoui R, Levaillant JM, Benoit B, Faro C, Wegrzyn P, Nicolaides KH. Three-dimensional sonographic description of abnormal metopic suture in second- and third-trimester fetuses. *Ultrasound Obstet Gynecol* 2005;26:761-64.
9. Kim MS, Jeanty P, Turner C, Benoit B. Three-dimensional sonographic evaluations of embryonic brain development. *J Ultrasound Med* 2008;27:119-24.
10. Hata T, Dai SY, Kanenishi K, Tanaka H. Three-dimensional volume-rendered imaging of embryonic brain vesicles using inversion mode. *J Obstet Gynaecol Res* 2009;35(2):258-61.
11. Blaas HG, Eik-Nes SH, Isaksen CV. The detection of spina bifida before 10 gestational weeks using two- and three-dimensional ultrasound. *Ultrasound Obstet Gynecol* 2000;16:25-29.
12. Nicolaides KH. Nuchal translucency and other first-trimester sonographic markers of chromosomal abnormalities. *Am J Obstet Gynecol* 2004;191:45-67.
13. Cicero S, Curcio P, Papageorghiou A, Sonek J, Nicolaides K. Absence of nasal bone in fetuses with trisomy 21 at 11-14 weeks of gestation: An observational study. *Lancet* 2001;358:1665-67.
14. Zoppi MA, Ibba RM, Axiana C, Floris M, Manca F, Monni G. Absence of fetal nasal bone and aneuploidies at first-trimester

- nuchal translucency screening in unselected pregnancies. *Prenat Diagn* 2003;23:496-500.
15. Cicero S, Rembouskos G, Vandecruys H, Hogg M, Nicolaides KH. Likelihood ratio for trisomy 21 in fetuses with absent nasal bone at the 11-14 weeks scan. *Ultrasound Obstet Gynecol* 2004;23:218-23.
 16. Cicero S, Avgidou K, Rembouskos G, Kagan KO, Nicolaides KH. Nasal bone in first-trimester screening for trisomy 21. *Am J Obstet Gynecol* 2006;195:109-14.
 17. Rembouskos G, Cicero S, Longo D, Vandecruys H, Nicolaides KH. Assessment of the fetal nasal bone at 11-14 weeks of gestation by three-dimensional ultrasound. *Ultrasound Obstet Gynecol* 2004;23:232-36.
 18. Benoit B, Chaoui R. Three-dimensional ultrasound with maximal mode rendering: A novel technique for the diagnosis of bilateral or unilateral absence or hypoplasia of nasal bones in second-trimester screening for Down syndrome. *Ultrasound Obstet Gynecol* 2005;25:19-24.
 19. Cicero S, Curcio P, Rembouskos G, Sonek J, Nicolaides KH. Maxillary length at 11-14 weeks of gestation in fetuses with trisomy 21. *Ultrasound Obstet Gynecol* 2004;24:19-22.
 20. Teoh M, Meagher S. First-trimester diagnosis of micrognathia as a presentation of Pierre-Robin syndrome. *Ultrasound Obstet Gynecol* 2003;21:616-68.
 21. Tsai MY, Lan KC, Ou CY, Chen JH, Chang SY, Hsu TY. Assessment of the facial features and chin development of fetuses with use of serial three-dimensional sonography and the mandibular size monogram in a Chinese population. *Am J Obstet Gynecol* 2004;190:541-46.
 22. Francis PJ, Berry V, Bhattacharya SS, Moore AT. The genetics of childhood cataract. *J Med Genet* 2000;37:481-88.
 23. Thut CJ, Rountree RB, Hwa M, Kingsley DM. A large-scale in situ screen provides molecular evidence for the induction of eye anterior segment structures by the developing lens. *Dev Biol* 2001;231:63-76.
 24. Karkinen-Jääskeläinen M, Saxen L, Vaheri A, Leinikki P. Rubella cataract in vitro: Sensitive period of the developing human lens. *J Exp Med* 1975;141:1238-48.
 25. Romain M, Awoust J, Dugauquier C, Van Maldergem L. Prenatal ultrasound detection of congenital cataract in trisomy 21. *Prenat Diagn* Aug 1999;19(8):780-82.
 26. Pedreira DA, Diniz EM, Schultz R, Faro LB, Zugaib M. Fetal cataract in congenital toxoplasmosis. *Ultrasound Obstet Gynecol* Apr 1999;13(4):266-67.
 27. Daskalakis G, Anastasakis E, Lyberopoulos E, Antsaklis A. Prenatal detection of congenital cataract in a fetus with Lowe syndrome. *J Obstet Gynaecol* 2010;30(4):409-10.
 28. Reches A, Yaron Y, Burdon K, Crystal-Shalit O, Kidron D, Malcov M, Tepper R. Prenatal detection of congenital bilateral cataract leading to the diagnosis of Nance-Horan syndrome in the extended family. *Prenat Diagn* 2007;27(7):662-64.
 29. Léonard A, Bernard P, Hiel AL, Hubinont C. Prenatal diagnosis of fetal cataract: Case report and review of the literature. *Fetal Diagn Ther* 2009;26(2):61-67. Epub 2009 Sep 11.
 30. Bolitho DG. Hand, congenital hand deformities. *emedicine* 2006. <http://www.emedicine.com/plastic/TOPICT298.HTM>
 31. Carbillon L, Seince N, Largillière C, Bucourt M, Uzan M. First-trimester diagnosis of sirenomelia: A case report. *Fetal Diagn Ther* 2001;16(5):284-88.
 32. Monteagudo A, Mayberry P, Rebarber A, Paidas M, Timor-Tritsch IE. Sirenomelia sequence: First-trimester diagnosis with both two- and three-dimensional sonography. *J Ultrasound Med* 2002;21:915-20.
 33. Schiesser M, Holzgreve W, Lapaire O, Willi N, Lüthi H, Lopez R, Tercanli S. Sirenomelia, the mermaid syndrome—detection in the first trimester. *Prenat Diagn* 2003;23:493-95.
 34. Dugoff L, Thieme G, Hobbins JC. First trimester prenatal diagnosis of chondroectodermal dysplasia (Ellis-van Creveld syndrome) with ultrasound. *Ultrasound Obstet Gynecol* 2001;17:86-88.
 35. Percin EF, Guvenal T, Cetin A, Percin S, Goze F, Arici S. First-trimester diagnosis of Robinow syndrome. *Fetal Diagn Ther* 2001;16:308-11.
 36. Doyle NM, Lally KP. The CDH study group and advances in the clinical care of the patient with congenital diaphragmatic hernia. *Semin Perinatol* 2004;28:174-84.
 37. Daskalakis G, Anastasakis E, Souka A, Manoli A, Koumpis C, Antsaklis A. First trimester ultrasound diagnosis of congenital diaphragmatic hernia. *J Obstet Gynaecol Res* 2007;33:870-72.